Proton-Coupled Electron Transfer in Guanine Oxidation: Effects of Isotope, Solvent, and Chemical Modification

Stephanie C. Weatherly, Ivana V. Yang, Paul A. Armistead, and H. Holden Thorp*

Department of Chemistry, University of North Carolina at Chapel Hill, Chapel Hill, North Carolina 27599-3290

Received: September 17, 2002; In Final Form: October 23, 2002

The proton-coupled electron-transfer reactions of guanine and other modified purine nucleobases have been investigated by electrochemistry and stopped-flow spectrophotometry. The rate of oxidation of guanine by $Ru(bpy)_3^{3+}$ varied linearly with the fraction of D_2O in H_2O/D_2O mixtures (bpy = 2,2′-bipyridine), suggesting the involvement of a single proton, consistent with earlier studies (Weatherly, S. C.; Yang, I. V.; Thorp, H. H. *J. Am. Chem. Soc.* **2001**, *123*, 1236−1237). The oxidation of the tetrabutylammonium salt of 2′-deoxyguanosine-5′-monophosphate was investigated in acetonitrile. The oxidants were polypyridyl complexes of Ru(III) and Fe(III) that ranged in oxidation potential from 0.83 to 1.6 V versus SCE. The values of (RT ln k) obtained for these reactions increased with driving force with a slope of 0.5 ± 0.1, consistent with a simple electron-transfer reaction. A conventional slope of 0.5 was not observed in aqueous solution where deprotonation of the guanine nucleobase was feasible. In addition to the driving force dependence, there was a dramatic suppression in the overall rate of guanine oxidation in acetonitrile compared to water both for dilute solution and for modified electrodes. The driving force dependence for the rate of oxidation of 7-deazaguanine and 7-deazaadenine was also investigated; plots of (RT ln k) versus $E_{1/2}$ showed slopes of 1.1 in aqueous solution, and these reactions gave large isotope effects ranging from 2.2 to 10, depending on the nucleobase and the oxidant. In contrast, the base 7,8-dihydro-8-oxoguanine did not exhibit an isotope effect, because the pK_a of this nucleobase is known to be near 7. Taken together, these results suggest a picture where oxidation of guanine in aqueous solution by these oxidants proceeds via concerted proton-coupled electron transfer.

Introduction

The coupling of a proton transfer to an electron transfer has a number of important implications for redox kinetics and thermodynamics.[1−7] If an electron transfer reaction produces for example an oxidized product that is acidic, then deprotonation of the oxidized species lowers the overall energy of the reaction according to the Nernst equation. Separation of the proton transfer and electron transfer events often leads to a first step that is highly unfavorable, such as (in the oxidation case) initial electron transfer to form a highly acidic oxidized species or initial proton transfer to form a strongly reducing deprotonated species. Thus, these processes generally occur via a concerted reaction, termed proton-coupled electron transfer (PCET, Scheme 1).[2,4,7] While these PCET reactions produce the energetically most favorable route, the need to release the proton often increases the kinetic barrier to the overall process. When the proton transfer and electron transfer are concerted, large isotope effects can also be observed for the PCET reaction.[5,6,8,9] Numerous experimental and theoretical studies on metal complexes have delineated the factors that control the kinetic barriers to the PCET process.[1−8]

Nucleobases, such as guanine, undergo PCET upon one-electron oxidation in neutral solution.[10−14] The mechanism of guanine oxidation is potentially relevant to aging and mutagenesis,[15,16] and other nucleobases, such as xanthine, undergo oxidative enzymatic transformations to which PCET processes may be relevant.[17] In addition, guanine has been used as a convenient internal donor for studies of DNA electron transfer.[18−22] Guanine can also act as a redox-active reporter for electrocatalytic reactions used in DNA sensing.[23] In such a system, guanine is oxidized by metal complexes, such as $Ru(bpy)_3^{3+}$ (bpy = 2,2′-bipyridine), whose reactive form is generated at the electrode to initiate a catalytic cycle:[24]

SCHEME 1

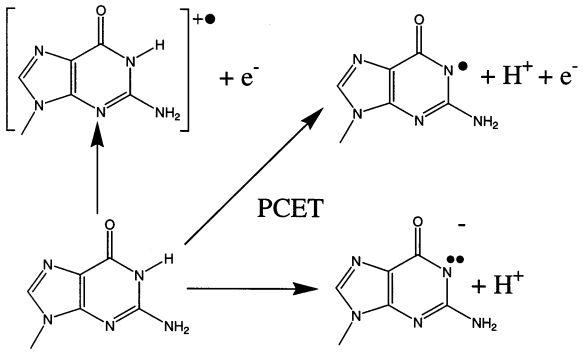

$$Ru(bpy)_3^{2+} \rightarrow Ru(bpy)_3^{3+} + e^- \quad (1)$$

$$Ru(bpy)_3^{3+} + \text{guanine} \rightarrow Ru(bpy)_3^{2+} + \text{“guanine}_{ox}\text{”} \quad (2)$$

where “guanine$_{ox}$” is a form of guanine that has been oxidized by one electron. Thus, the kinetics of guanine−$Ru(bpy)_3^{3+}$

* Corresponding author.

10.1021/jp022085r CCC: $25.00
Published on Web 12/06/2002

electron transfer can be monitored either by cyclic voltammetry and subsequent digital simulation of the electrocatalytic signal or by stopped-flow spectrophotometry where guanine-containing species are mixed with an authentic sample of $Ru(bpy)_3^{3+}$.[14,24−26]

We recently reported on initial studies of PCET reactions between guanine and metal complexes based on $Ru(bpy)_3^{3+}$.[14] These studies showed that eq 2 proceeds with an isotope effect of about 2, implicating the importance of a proton transfer event in the reaction; these observations are consistent with cleavage studies by Giese and Wessely[11] and photochemical measurements by Shafirovich et al.[10] Our earlier investigations also showed that the dependence of the rate of eq 2 on driving force in H_2O gave a Marcus plot of ($RT \ln k$) versus $E_{1/2}$ of the metal oxidant with a slope of 0.8 ± 0.1.[14] For simple electron transfers, theory predicts that the Marcus plot will have a slope of 0.5.[27] The elevated slope observed for eq 2 was attributed to the involvement of the proton in the reaction.

The high slope of the Marcus plot for eq 2 was observed for guanine mononucleotides, single-stranded oligonucleotides containing guanine, duplex oligonucleotides containing guanine, and genomic DNA.[14] Similarly, the isotope effect was also observed for both duplex and mononucleotide forms. Thus, the PCET reaction occurs for guanine that is highly accessible to the solvent and for guanine that is enclosed in the double helix and base-paired to cytosine. In duplex DNA, the initial transfer of a proton to cytosine is a possibility,[11] although the slower time scale of our thermal reactions may allow for initial transfer to solvent. Transfer of the proton to the solvent is not necessarily available in photoinduced oxidations that occur on much faster time scales.[19,28] These studies address an important general question in biological electron-transfer involving redox sites that are buried in biomolecules but that require proton transfer to undergo oxidation. This question pertains to oxidation of buried organic sites in proteins in addition to DNA oxidation.[29] In our case, it appears that the guanine is able to transfer its proton to the solvent from within the double helix on a time scale that allows for coupling of the electron and proton transfers. This finding is consistent with related studies showing that tyrosine and tryptophan residues, which become acidic upon oxidation, readily deprotonate from within the hydrophobic cores of redox proteins.[30]

In this paper, we present additional information that supports the observation of PCET for guanine under a variety of conditions. Carrying out eq 2 in acetonitrile solution where proton transfer is prohibited results in a dramatic decrease in the rate of guanine oxidation, as expected when the reaction is forced to proceed to the radical cation instead of the more stable deprotonated form (Scheme 1). This result is obtained both in acetonitrile solution and with DNA-modified electrodes placed in acetonitrile. In addition, 7-deazapurines, which are excellent donors that undergo electron transfer to $Ru(bpy)_3^{3+}$ or even less oxidizing complexes,[31,32] give Marcus plots with elevated slopes that are different for each donor and give different isotope effects for each reaction. Finally, the isotope effect for eq 2 is shown to arise from involvement of a single proton. These observations all support the oxidation of guanine and 7-deazapurines by PCET where the intimate chemistry of the oxidized moiety controls the Marcus slope and kinetic isotope effect.

Experimental Section

Highly polymerized calf-thymus and herring-testes DNA were purchased from Sigma and sheared by repeated sonication and passage through a 22-gauge needle. 2′-Deoxy-8-oxoguanosine 5′-monophosphate (8-oxodGMP) was synthesized and purified according to a published protocol.[33] The 2′-deoxyguanosine 5′−monophosphate in the free acid form (H_2dGMP) was purchased from Sigma. Tetrabutylammonium hydroxide, 31% in methanol (TBAOH) was obtained from Alfa Aesar. dGTP, 7-deaza-dATP and 7-deaza-dGTP were obtained from Pharmacia and Roche and used as received. Water was purified with a MilliQ purification system (Millipore), and D_2O (99.9 atom %) was purchased from Aldrich. Spectroscopic grade acetonitrile was obtained from Burdick and Jackson. Tetrabutylammonium hexafluorophosphate (TBAH) and lithium perchlorate were purchased from Aldrich and used without further purification. Sodium phosphate, sodium acetate, magnesium sulfate, and sodium chloride were from Mallinckrodt and used without further purification. Na_2DPO_4 and NaD_2PO_4 were prepared by dissolving Na_2HPO_4 and NaH_2PO_4 in D_2O, followed by evaporation of the solvent. The relation $pD = pH_{read} - 0.4$ was used to determine pD values of the buffer solutions.[34] ITO electrodes were purchased from Delta Technologies, and vitreous carbon electrodes were purchased from Electrosynthesis Co., Inc. $Ru(bpy)_3Cl_2$ was purchased from Aldrich and was recrystallized from acetonitrile. $Ru(bpy)_3(PF_6)_2$ was prepared by dissolving $Ru(bpy)_3Cl_2$ in water and precipitating it using excess ammonium hexafluorophosphate (Aldrich).

$[Ru(bpm)_3](PF_6)_2$ was prepared according to a literature procedure (bpm = bipyrimidine).[35] Literature procedures were also followed to prepare polypyridyl complexes of ruthenium(II),[36] iron(II),[37] and osmium(II).[32] Metal(III) complexes were synthesized by oxidation of the corresponding metal(II) complexes according to a published protocol.[37]

$(TBA)_2$dGMP. The free acid mononucleotide of dGMP was converted to the corresponding tetrabutylammonium salt by neutralizing the free acid with two equivalents of TBAOH. As an example, 0.05 g of H_2dGMP was combined with 0.23 g of TBAOH in a round-bottomed flask. Approximately 3 mL of methanol were added to wash any solid dGMP off of the sides of the flask. The H_2dGMP dissolved completely in the TBAOH, and this solution was then dried by rotary evaporation. A colorless, oily residue was left on the sides of the flask that was washed in 5 mL of CH_3CN and dried by rotary evaporation three times. The final residue was dissolved in 10 mL of CH_3CN, and 0.5 g $MgSO_4$ was added to dry the solution. The $MgSO_4$ was filtered out, and the filter and filtrate were rinsed with 10 mL of CH_3CN. The concentration of TBA_2-dGMP was calculated using the number of moles of initial mononucleotide in 20 mL CH_3CN. The concentration of mononucleotide agreed with that calculated by measuring the absorbance of the mononucleotide using the absorption maximum and extinction coefficient determined for the monucleotide in water.[38]

Stopped-Flow Spectrophotometry. Kinetic experiments were carried out using an On Line Instrument Systems OLIS RSM-1000 stopped-flow system. The reaction was monitored spectrophotometrically at λ_{max} of the metal complex in the reduced form (M^{2+}) $\pm$ 230 nm. Solutions were maintained at 25 ± 1 °C. Aqueous experiments were conducted by dissolving the oxidant in ~10 mM H_2SO_4 or DCl with 800 mM NaCl (pH 2) and by dissolving the DNA in pH 8 phosphate buffer with 800 mM NaCl to give a final solution that was 50 mM sodium phosphate, pH 7 with 800 mM NaCl. Nonaqueous stopped flow experiments were conducted by dissolving the oxidized metal species in 0.05 M $LiClO_4/CH_3CN$. $Ru(bpm)_3^{3+}$ was generated electrochemically by bulk electrolysis of a solution of Ru-

$(bpm)_3^{2+}$ in 0.05 M $LiClO_4/CH_3CN$ that was held at 1.6 V (Ag wire reference, Pt wire counter, vitreous carbon working electrode). An aliquot of the Ru^{3+} solution was removed for each experiment and used immediately. TBA_2dGMP was diluted to 1 mM with 0.05 M $LiClO_4/CH_3CN$.

Second-order oxidation rate constants were determined by global analysis[39] of all the data using the SPECFIT software (Spectrum Software Associates, Chapel Hill). The data were fit to either the mechanism described by eq 3 or the 2-population mechanism described by eqs 4 and 5:

$$M^{3+} + DNA \rightarrow M^{2+} + DNA_{ox} \quad (3)$$

$$M_A^{3+} + DNA \rightarrow M^{2+} + DNA_{ox} \quad (4)$$

$$M_B^{3+} + DNA \rightarrow M^{2+} + DNA_{ox} \quad (5)$$

The initial concentrations of M^{2+} and M^{3+} were determined from the stopped-flow data. $[M^{2+}] = A_{min}/b^* \epsilon_{M2+}$ and $[M^{3+}] = A_{max} - A_{min} / b^* \epsilon_{M2+}$ where A_{max} is the maximum absorbance at the wavelength of interest, A_{min} is the minimum absorbance, b is the cell path length (1.8 cm), and ϵ_{M2+} is the extinction coefficient for M^{2+}. The two-population mechanism that we have described previously[40] was used with a 1:1 ratio of M_A^{3+} to M_B^{3+}.

Proton Inventory Experiment. Cyclic voltammetry experiments were performed on either an EG&G Princeton Applied Research potentiostat model 273A or a Bioanalytical Systems potentiostat model 100B. ITO electrodes were cleaned by sonicating 10 min in 2-propanol, followed by two, 10-min washes in water. ITO electrodes were allowed to air-dry overnight. Cyclic voltammograms were collected at 25 mV/s with a Ag/AgCl reference electrode and a Pt wire counter electrode in an apparatus previously described.[41] The potential was swept from 0 to 1.3 V. The ITO electrode was conditioned for 6 cycles in 50 mM sodium phosphate (pH, pD = 7), 800 mM NaCl, and then a background cyclic voltammogram of the sodium phosphate buffer alone was obtained. The buffer was removed from the cell and a solution of 50 μM ruthenium was introduced. A cyclic voltammogram of the ruthenium solution was obtained and then this ruthenium solution was replaced with a solution containing either 50 μM Ru and 25 μM dGMP or 50 μM Ru and 1 mM ht DNA. After the cyclic voltammogram of the Ru + DNA (or dGMP) solution was obtained, the ITO electrode was discarded and a fresh ITO was used for each subsequent experiment. The background for the buffer alone was subtracted from the voltammograms of both the ruthenium only and the Ru + DNA (or dGMP) cyclic voltammogram. All solutions were made in 50 mM sodium phosphate (pH, pD = 7), 800 mM NaCl. The D_2O/H_2O mixtures were obtained by mixing the D_2O or H_2O solutions of 50 mM sodium phosphate (pH, pD = 7), 800 mM NaCl.

Digital simulations were performed using the DigiSim software package (BAS).[42] Guanine concentrations were used in the fit (25% of the total ht DNA concentration). The diffusion coefficients used were 6×10^{-6} cm^2/s for $Ru(bpy)_3^{2+/3+}$,[24] and 2×10^{-7} cm^2/s for ht DNA.[43] The diffusion coefficient for dGMP was assumed to be 6×10^{-6} cm^2/s. The reduction potential of $Ru(bpy)_3^{3+}$, the electrode area, and the heterogeneous electron-transfer rate constant were obtained by fitting the voltammogram of $Ru(bpy)_3^{2+}$ alone in solution. The rate constants (k_1, k_2, k_3) for the DNA oxidation were obtained by fitting the Ru + DNA (or dGMP) cyclic voltammogram. The mechanism was as follows:

$$Ru^{3+} \rightarrow Ru^{2+} \quad (6)$$

$$Ru^{3+} + e^- \rightarrow Ru^{2+} \quad (7)$$

$$Ru^{3+} + G \rightarrow Ru^{2+} + G' \ (k_1) \quad (8)$$

$$Ru^{3+} + G' \rightarrow Ru^{2+} + G'' \ (k_2) \quad (9)$$

$$Ru^{3+} + G'' \rightarrow Ru^{2+} + G''' \ (k_3) \quad (10)$$

The three second-order rate constants are then used to generate a Ru^{2+} concentration profile that is fit by SPECFIT software. This analysis produces a single second-order rate constant for the oxidation reaction.

DNA-Modified Electrodes. The DNA-modified electrodes were prepared according to published procedures.[44] Aqueous electrochemical measurements were performed in a one-compartment electrochemical cell that held 4 mL of solution. The cell had a platinum coil as the auxiliary electrode and a silver wire as a quasi reference electrode. All cyclic voltammograms in aqueous solution were swept from 0 to 1.3 V vs the silver wire quasi-reference. Background cyclic voltammograms were acquired by using cleaned, unmodified ITO electrodes in 50 mM sodium phosphate (pH = 7.0). These were acquired at a scan rate of 10 V/s. Cyclic voltammograms of DNA-modified electrodes were also taken in phosphate buffer at the same scan rate. The concentration of Ru(II) complex was 25 μM in 50 mM sodium phosphate (pH = 7.0). The $E_{1/2}$ measurements taken for both metal complexes at 100 mV/s on unmodified ITO electrodes were compared to their known $E_{1/2}$ values versus NHE. This comparison served to calibrate the potentials measured by the silver wire quasi-reference electrode to NHE. Nonaqueous electrochemical experiments were performed with the same electrochemical cell and electrodes in acetonitrile with 100 mM TBAH.

Results

Oxidation of Guanine in Acetonitrile Solution. As discussed above, we observed previously that guanine oxidation in water gave a slope for the Marcus plot of 0.8 ± 0.1,[14] which was significantly higher than the expected value of 0.5. If this elevated slope results from PCET, then we expect that the slope of the Marcus plot should return to a normal value of 0.5 when proton transfer was not available. We therefore prepared the tetrabutylammonium salt of deoxyguanosine 5′-monophosphate (dGMP), which was soluble in acetonitrile. The rates of $(TBA)_2dGMP$ oxidation by a series of substituted Ru complexes were measured in CH_3CN using stopped-flow spectrophotometry. As observed previously for aqueous solution,[14,40] the kinetics follow a double-exponential, but both components exhibit the same dependence on driving force and solvent. The measured rate constants are about 30 times slower than those measured for the same complexes in water: for the reactions of $Ru(bpy)_3^{3+}$ with dGMP, the rate of the fast component was $(2.3 \pm 0.4) \times 10^6$ M^{-1} s^{-1} in water and $(7.22 \pm 0.67) \times 10^4$ in acetonitrile under the same conditions. Apparently, the absence of a proton acceptor forces the reaction to proceed uphill to the protonated radical cation, dramatically slowing the reaction.

The rate constants obtained with the series of Ru complexes are shown in Table 1 (the rate constants reported are those for the faster of the two components of the double exponential).

TABLE 1: Rate Constants for Oxidation of dGMP in Acetonitrile

oxidant ($E_{1/2}$ versus SSCE)	k (M^{-1} s^{-1})
$Fe(bpy)_3^{3+}$ (0.83 V)	$(1.59 \pm 0.24) \times 10^2$
$Ru(dmb)_3^{3+}$ (0.86 V)[a]	$(2.67 \pm 0.58) \times 10^3$
$Ru(dmb)_2(bpy)^{3+}$ (0.93 V)	$(1.00 \pm 0.37) \times 10^4$
$Ru(dmb)(bpy)_2^{3+}$ (0.97 V)	$(3.82 \pm 0.51) \times 10^4$
$Ru(bpy)_3^{3+}$ (1.05 V)	$(7.22 \pm 0.67) \times 10^4$
$Ru(bpm)_3^{3+}$ (1.6 V)[b]	$(1.34 \pm 0.68) \times 10^5$

[a] dmb = 4,4′-dimethyl-2,2′-bipyridine. [b] bpm = 2,2′-bipyrimidine.

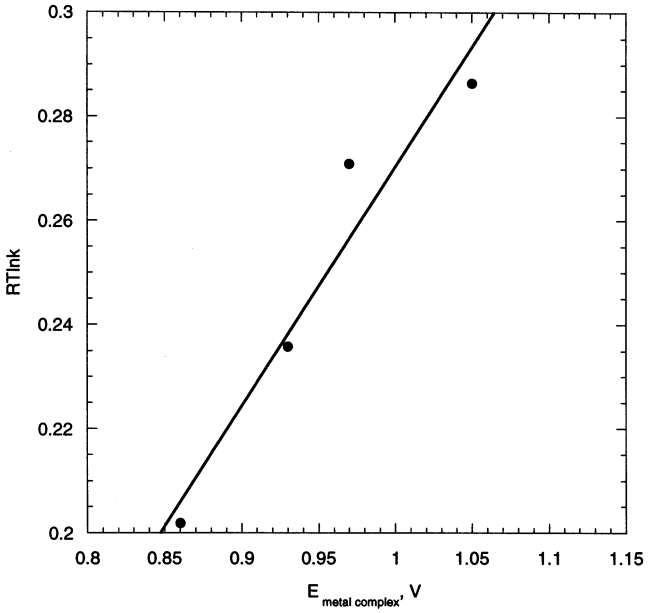

Figure 1. Marcus plot for the driving force dependence of TBA_2dGMP oxidation in CH_3CN. Rate constants were obtained from stopped-flow spectrophotometry. These data represent the linear region of the Marcus plot, the slope of the line is 0.5 ± 0.09.

The rate constants exhibit a Rehm−Weller dependence,[45] with increasing rate constants at low driving force that level off at higher driving force. At low driving force, the plot of rate constant as a function of redox potential (the redox potentials used for the Ru complexes are the aqueous potentials) has a slope of 0.5 ± 0.09 (Figure 1). The rate is apparently controlled solely by the electron-transfer reaction, giving a conventional value for the slope. This result supports the suggestion that the elevated slopes obtained in H_2O for the different guanine species are a result of mixed control of the deprotonation equilibrium and the oxidation reaction.

Oxidation of Guanine-Modified Electrodes in Acetonitrile. We have developed a protocol for attaching polymeric nucleic acids to indium tin oxide (ITO) electrodes based on adsorption from DMF/acetate.[44,46] Cyclic voltammograms of these DNA-modified electrodes show very little direct current for guanine oxidation in aqueous buffer only (Figure 2A, dotted), but show large current enhancements in the presence of $Ru(bpy)_3^{2+}$ (Figure 2A, solid). This large current comes from catalytic oxidation of the guanine in surface-attached DNA by the electrogenerated $Ru(bpy)_3^{3+}$.[44,46]

The DNA-modified electrodes were placed in acetonitrile solution containing supporting electrolyte and scanned by cyclic voltammetry under the same conditions where large current enhancements were obtained when the electrodes were placed in aqueous electrolyte. In acetonitrile, the current obtained with $Ru(bpy)_3^{2+}$ at modified electrodes (Figure 2B, solid) was simply the sum of the current for DNA-modified electrodes scanned in acetonitrile without $Ru(bpy)_3^{2+}$ (dotted) plus the current for

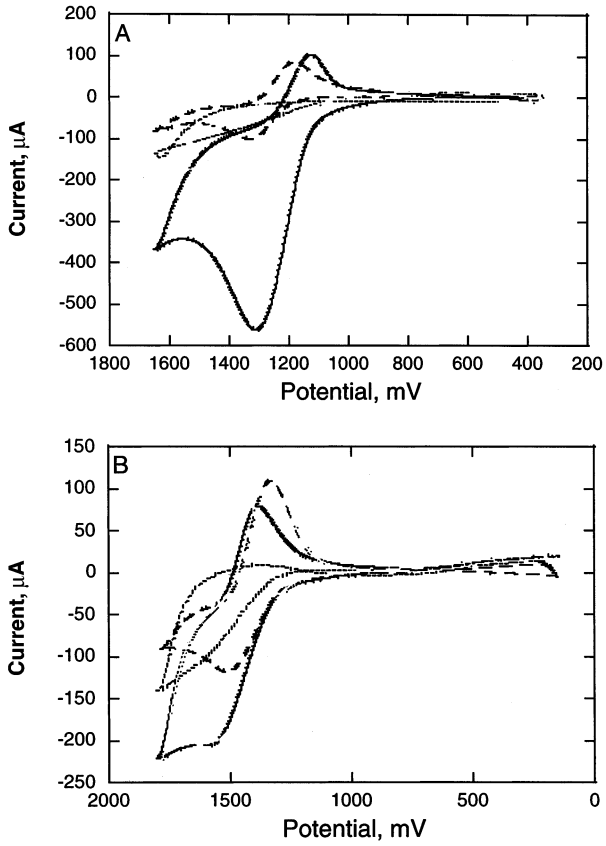

Figure 2. (A) Cyclic voltammograms at 10 V/s of indium-oxide electrodes in 50 mM sodium phosphate (pH = 7.0) with 25 μM $Ru(bpy)_3^{2+}$ (dashed), modified with DNA and scanned in buffer only (dotted), and modified with DNA and scanned in the presence of $Ru(bpy)_3^{2+}$ (solid). (B) Cyclic voltammograms at 10 V/s of indium oxide in acetonitrile with 100 mM TBAH and 25 μM $Ru(bpy)_3^{2+}$ (dashed), modified with DNA and scanned in the absence of $Ru(bpy)_3^{2+}$ (dotted), and modified with DNA and scanned in the presence of $Ru(bpy)_3^{2+}$.

the unmodified electrode with $Ru(bpy)_3^{2+}$ (dashed). Thus, there was no evidence for catalytic oxidation. Note the cyclic voltammograms of DNA-modified electrodes in acetonitrile alone show considerably more direct current for the irreversible oxidation of the guanine bases. The inability of the guanine base to deprotonate in acetonitrile strongly attenuates the guanine oxidation in polymeric DNA molecules on the ITO surface, as described above for dGMP in acetonitrile solution.

Oxidation of Deazapurines. As we and others have discussed,[31,32] 7-deazaguanine and 7-deazaadenine are effective electron donors to $Ru(bpy)_3^{3+}$ and related complexes. To understand further the origins of the high Marcus slope observed for guanine, the driving force dependence for the rate of oxidation of the 7-deaza analogues of guanine and adenine was also investigated. The observed rates of electron transfer for the faster and the slower reaction components for oxidation of 7-deaza-dGTP are summarized in Table 2. The reactions with metal complexes whose redox potentials are higher than that of 7-deazaguanine were too fast to be monitored by stopped-flow spectrophotometry. Rate constants for the oxidation of 7-deaza-dATP were also measured and are included in Table 2.

Plots of (RT ln k_{ET}) versus the redox potential of the metal complex for the faster and the slower reaction components for oxidation of 7-deaza-dGTP, 7-deaza-dATP, and dGTP are shown in Figure 3. As in the guanine case, the data for 7-deazaguanine and 7-deazaadenine fit well to a straight line. The mean value of the slopes for the two reaction components

TABLE 2: Second-Order Rate Constants for Oxidation of 7-Deazapurines

	rate constant, M^{-1} s^{-1}			
oxidant	7-deaza-dGTP k_1	7-deaza-dGTP k_2	7-deaza-dATP k_1	7-deaza-dATP k_2
$Os(dmb)_3^{3+}$	44 ± 6.0	4.8 ± 0.40	-[a]	-[a]
$Os(dmb)(bpy)_2^{3+}$	630 ± 15	53 ± 3.0	-[a]	-[a]
$Os(bpy)_3^{3+}$	$(1.2 \pm 0.10)\ 10^4$	920 ± 110	-[a]	-[a]
$Fe(dmb)_3^{3+}$	$(1.5 \pm 0.13)\ 10^5$	$(1.8 \pm 0.14)\ 10^4$	-[c]	-[c]
$Fe(bpy)_3^{3+}$	-[b]	-[b]	810 ± 93	190 ± 76
$Ru(dmb)_3^{3+}$	-[b]	-[b]	$(1.8 \pm 0.40)\ 10^3$	680 ± 200
$Ru(dmb)_2(bpy)^{3+}$	-[b]	-[b]	$(1.1 \pm 0.20)\ 10^5$	$(9.0 \pm 2.4)\ 10^3$
$Ru(dmb)(bpy)_2^{3+}$	-[b]	-[b]	$(1.2 \pm 0.30)\ 10^6$	$(1.6 \pm 0.40)\ 10^5$
$Ru(bpy)_3^{3+}$	-[b]	-[b]	$(3.9 \pm 1.3)\ 10^7$	$(3.2 \pm 1.1)\ 10^5$

[a] Reaction was too slow to be monitored. [b] Reaction was too fast to be monitored. [c] Rate not measured.

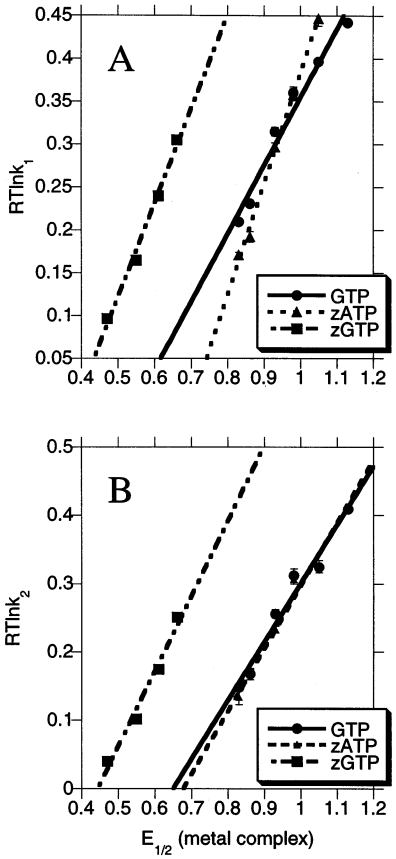

Figure 3. Plots of (RT ln k_{ET}) versus the redox potential of the metal complex for the (A) faster and (B) slower components for oxidation of guanine and 7-deaza analogues of guanine and adenine in mononucleotide triphosphate forms. Solid lines are best linear fits to the data points.

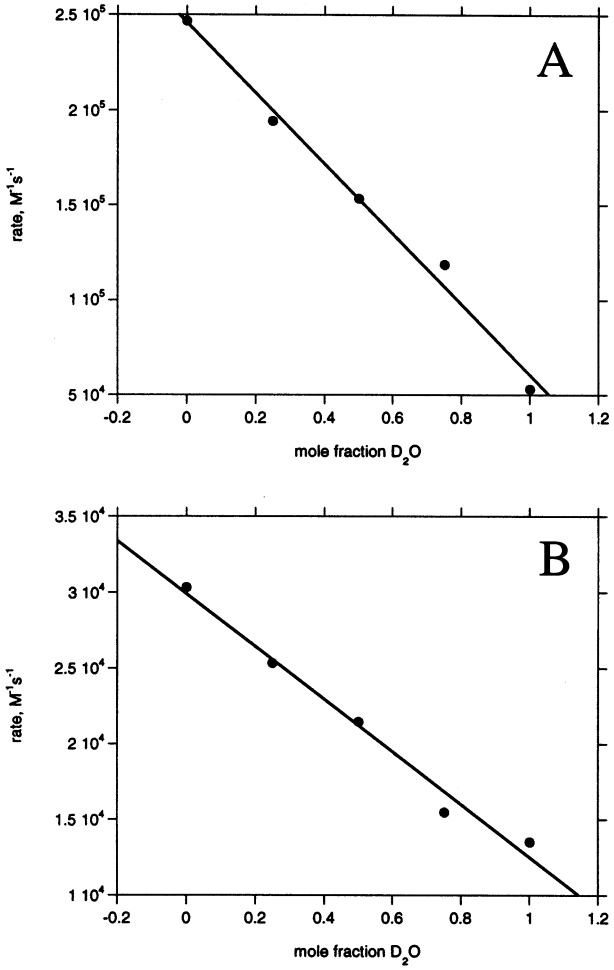

Figure 4. Electron-transfer rate constants obtained by fitting cyclic voltammograms of (A) 25 μM dGMP and 50 μM $Ru(bpy)_3^{2+}$ (B) 1 mM ht DNA and 50 μM $Ru(bpy)_3^{2+}$ in 50 mM sodium phosphate (pH = pD = 7), 800 mM NaCl with varying percentages of D_2O.

is 1.1 for both 7-deazaguanine and 7-deazaadenine. These slopes are even higher than the value of 0.8 observed for guanine. Thus, while changing the secondary structure context of the guanine did not change the value of the Marcus slope, changing the chemical nature of the donor did alter the slope. This result suggests that the high slope is a result of asymmetry in the transition state that arises from the involvement of the proton and the fundamental acid−base and redox chemistry of the donor.

Isotope Effects. We have published previously that the oxidation of guanine in both DNA and dGMP proceeds with a kinetic isotope effect of 1.4−2.1.[14] Like the Marcus slope, the isotope effect is roughly independent of whether the guanine is in a free mononucleotide or hydrogen-bonded in duplex DNA. For these reactions, if a single proton is involved in the reaction, the rate constant should exhibit a linear dependence on the quantity of isotope present.[47] Figure 4 shows plots of the rate constants for oxidation of both dGMP and herring testes DNA by $Ru(bpy)_3^{3+}$ determined by digital simulation of cyclic voltammograms at 0, 25%, 50%, 75%, and 100% D_2O. As expected, both plots exhibit a linear dependence on the percentage of isotope in the reaction. Thus, the isotope effect results from the involvement of a single proton in the reaction, and again, this degree of involvement is independent of the secondary structure context of the guanine.

As with native guanine, oxidation of 7-deazapurines should be slower in D_2O than in H_2O if the proton loss is a part of the rate-determining step. The rate constants for oxidation of 7-deaza-dGTP and 7-deaza-dATP were determined in D_2O and

TABLE 3: Kinetic Isotope Effects for Oxidation of Deazapurines

substrate	oxidant	KIE k_1	KIE k_2	⟨KIE⟩[c]
7-deaza-dGTP	$Os(dmb)(bpy)_2^{3+}$	3.2 ± 0.46	2.2 ± 0.46	2.7
7-deaza-dGTP	$Os(bpy)_3^{3+}$	2.7 ± 0.38	2.2 ± 0.78	2.5
7-deaza-dGTP	$Fe(dmb)_3^{3+}$	5.4 ± 1.2	10 ± 2.1	7.7
7-deaza-dATP	$Ru(dmb)_3^{3+}$	3.0 ± 1.3	-[a]	-
7-deaza-dATP	$Ru(dmb)_2(bpy)^{3+}$	5.7 ± 3.2	4.3 ± 2.3	5.0
7-deaza-dATP	$Ru(dmb)(bpy)_2^{3+}$	10 ± 3.4	-[b]	-

[a] Fit to single exponential. [b] Could not be determined accurately due to large errors in the observed rate constants. [c] $\langle KIE \rangle = (\text{KIE } k_1 + \text{KIE } k_2)/2$.

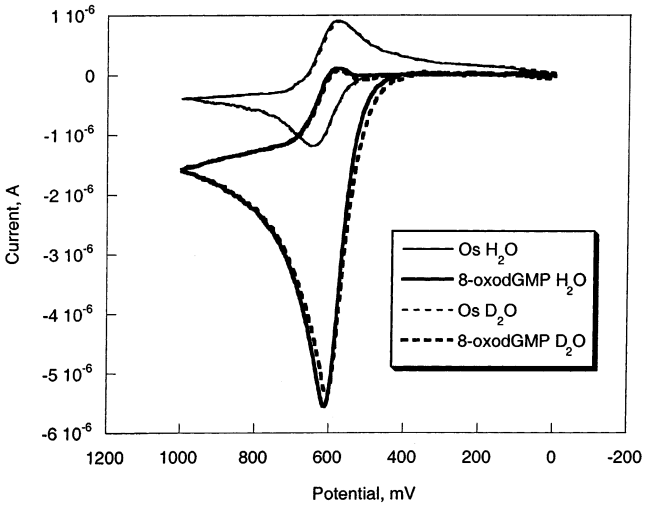

Figure 5. Cyclic voltammograms of 100 μM 8-oxodGMP and 50 μM $Os(bpy)_3^{2+}$ in 50 mM sodium phosphate (pH, pD = 7), 800 mM NaCl. Cyclic voltammograms were collected at 25 mV/s on ITO working electrode with Ag/AgCl reference, and Pt wire counter electrode. Data collected in D_2O are shown with a dashed line. Data collected in H_2O are shown with a solid line.

used to calculate isotope effects on both the fast (k_1) and slow (k_2) components of each reaction (Table 3). The observed kinetic isotope effects for both 7-deaza analogues roughly increased with the increasing driving force. These results again suggest that the kinetic parameters are much more sensitive to the intimate chemistry of the donor, which would be expected to influence the transition-state symmetry.

The kinetic isotope effect of $Os(bpy)_3^{3+}$-mediated oxidation of 8-oxodGMP was also examined by cyclic voltammetry. Because the 8-oxo$G^{\bullet+}$ species has a pK_a of 6.6,[12] we did not expect to see a significant isotope effect at neutral pH. Figure 5 shows the cyclic voltammograms of $Os(bpy)_3^{2+}$ and 8-oxodGMP in D_2O and H_2O. Unlike dGMP, the cyclic voltammograms overlay each other, suggesting that there is no decreased rate in D_2O. Since the 8-oxo$G^{\bullet+}$ is not a particularly strong acid, this observation supports our assignment of the isotope effect for dGMP to proton-coupled electron transfer.

Discussion

Mechanism of PCET. Recent theoretical efforts show that a number of factors control the kinetics of PCET reactions.[2,4] In particular, the proton-transfer distance is a large determinant of the kinetic isotope effect as is the coupling of the electronic states of the reactant and product.[5,6] This effect arises because when the proton is involved in the reaction, higher vibrational states for the product may contribute to the overall rate much more than in the simple electron transfer case. The cases studied theoretically are those where both the proton and electron are transferred from one molecule to another.[5,6] In our case, the electron is transferred from the nucleobase to the metal complex, and the proton is transferred from the nucleobase to the solvent.

The systems where the proton is transferred to the same molecule that receives the electron are much simpler to constrain geometrically and hence to analyze theoretically; however, some generalities from the simpler systems apparently apply to our guanine oxidation.[5,6] Namely, the ground vibrational state of the product may not predominate, causing deviations in the slope of the Marcus plot from the expected value of 0.5. In our system, the ground vibrational state of the product may have poor overlap with the reactant state, causing a higher vibrational state to dominate the overall rate. This could lead to the high slopes in the driving force plots and to the relatively large kinetic isotope effects in some cases. Additionally, the derivatives with different $E_{1/2}$ values may exhibit different degrees of overlap for the relevant vibrational states, causing different apparent slopes in the driving force plots. This effect would cause the driving force plots to deviate from linearity, but given the limited number of available experimental data points, such a deviation may be difficult to discern.

In our original paper, we suggested that *separate* proton and electron-transfer steps could give rise to the high slopes of the driving force plots;[14] this reasoning would apply most appropriately to reactions where the ground proton and electron vibrational states predominate and Marcus theory remains in effect. The new theoretical and experimental evidence suggests that *concerted* PCET reactions can exhibit high slopes and kinetic isotope effects.[5,6] Evidence that supports such an assignment here is the fact that different slopes are observed for guanine, 7-deazaguanine, and 7-deazaadenine, and that different isotope effects are observed for each nucleobase−oxidant pair. Further, these isotope effects are in some cases as high as 10, suggesting an important role for excited proton vibrational states. Thus, changes in the chemical nature of the nucleobase, which profoundly affect the energies and overlaps of the relevant electron and proton states, control the slopes and isotope effects. In contrast, the secondary structure context, i.e., whether the nucleobase is single-stranded or double-stranded, does not affect the slopes and isotope effects. This evidence therefore supports a concerted PCET reaction.

Role of Biomolecular Structure in PCET. These studies also address the general question of whether an oxidized moiety encapsulated in a biomolecule can deprotonate in concert with electron transfer.[29] In addition to guanine in DNA, this issue applies to tyrosine and tryptophan residues that might be buried in protein interiors without nearby bases to accept protons.[30] In these cases, the tyrosine residues are able to transfer protons to solvent concomitantly with electron transfer to electron acceptors. Similarly, we find that the slope, isotope effect, and number of protons involved in the reaction for guanine oxidation are the same for either duplex or single-stranded DNA. Thus, the guanine base is able to exchange protons with solvent on a time scale compatible with the electron transfer. Similar results have been obtained by laser flash photolysis in a different system.[10]

Acknowledgment. We thank Professor Sharon Hammes-Schiffer for enlightening discussions. This research was supported by Xanthon, Inc.

References and Notes

(1) Roth, J. P.; Lovell, S.; Mayer, J. M. *J. Am. Chem. Soc.* **2000**, *122*, 5486−5498.

(2) Cukier, R. I.; Nocera, D. G. *Annu. Rev. Phys. Chem.* **1998**, *49*, 337−369.

(3) Turro, C.; Zaleski, M.; Karabatsos, Y. M.; Nocera, D. G. *J. Am. Chem. Soc.* **1996**, *118*, 6060−6067.
(4) Hammes-Schiffer, S. *Acc. Chem. Res.* **2001**, *34*, 273−281.
(5) Iordanova, N.; Decornez, H.; Hammes-Schiffer, S. *J. Am. Chem. Soc.* **2001**, *123*, 3723−3733.
(6) Iordanova, N.; Hammes-Schiffer, S. *J. Am. Chem. Soc.* **2002**, *124*, 4848−4856.
(7) Meyer, T. J. *J. Electrochem. Soc.* **1984**, *131*, 221C.
(8) Farrer, B. T.; Thorp, H. H. *Inorg. Chem.* **1999**, *38*, 2497−2502.
(9) Stultz, L. K.; Binstead, R. A.; Reynolds, M. S.; Meyer, T. J. *J. Am. Chem. Soc.* **1995**, *117*, 2520−2532.
(10) Shafirovich, V.; Dourandin, A.; Geacintov, N. E. *J. Phys. Chem. B* **2001**, *105*, 8431−8435.
(11) Giese, B.; Wessely, S. *Chem. Commun.* **2001**, 2108−2109.
(12) Steenken, S.; Jovanovic, S. V.; Bietti, M.; Bernhard, K. *J. Am. Chem. Soc.* **2000**, *122*, 2373−2374.
(13) Steenken, S.; Jovanovic, S. V. *J. Am. Chem. Soc.* **1997**, *119*, 617−618.
(14) Weatherly, S. C.; Yang, I. V.; Thorp, H. H. *J. Am. Chem. Soc.* **2001**, *123*, 1236−1237.
(15) Helbock, H. J.; Beckman, K. B.; Shigenaga, M. K.; Walter, P. B.; Woodall, A. A.; Yeo, H. C.; Ames, B. N. *Proc. Natl. Acad. Sci. U.S.A.* **1998**, *95*, 288−293.
(16) Henle, E. S.; Han, Z. X.; Tang, N.; Rai, P.; Luo, Y. Z.; Linn, S. *J. Biol. Chem.* **1999**, *274*, 962−971.
(17) Hille, R. *Chem. Rev.* **1996**, *96*, 2757−2816.
(18) Schuster, G. B. *Acc. Chem. Res.* **2000**, *33*, 253−260.
(19) Lewis, F. D.; Liu, X.; Liu, J.; Hayes, R. T.; Wasielewski, M. R. *J. Am. Chem. Soc.* **2000**, *122*, 12037−12038.
(20) Hall, D. B.; Holmlin, R. E.; Barton, J. K. *Nature* **1996**, *382*, 731−735.
(21) Giese, B.; Biland, A. *Chem. Commun.* **2002**, 667−672.
(22) Grinstaff, M. W. *Angew. Chem., Int. Ed. Engl.* **1999**, *38*, 3629−3635.
(23) Thorp, H. H. *Trends Biotechnol.* **1998**, *16*, 117−121.
(24) Johnston, D. H.; Glasgow, K. C.; Thorp, H. H. *J. Am. Chem. Soc.* **1995**, *117*, 8933−8938.
(25) Szalai, V. A.; Thorp, H. H. *J. Phys. Chem. B* **2000**, *104*, 6851−6859.
(26) Sistare, M. F.; Holmberg, R. C.; Thorp, H. H. *J. Phys. Chem. B* **1999**, *103*, 10718−10728.
(27) Marcus, R. A.; Sutin, N. *Biochim. Biophys. Acta* **1985**, *811*, 265−322.
(28) Angelov, D.; Spassky, A.; Berger, M.; Cadet, J. *J. Am. Chem. Soc.* **1997**, *119*, 11373−11380.
(29) Chan, S. I.; Li, P. M. *Biochemistry* **1990**, *29*, 1−12.
(30) Di Bilio, A. J.; Crane, B. R.; Wehbi, W. A.; Kiser, C. N.; Abu-Omar, M. M.; Carlos, R. M.; Richards, J. H.; Winkler, J. R.; Gray, H. B. *J. Am. Chem. Soc.* **2001**, *123*, 3181−3182.
(31) Kelley, S. O.; Barton, J. K. *Chem. Biol.* **1998**, *5*, 413−425.
(32) Yang, I. V.; Thorp, H. H. *Inorg. Chem.* **2001**, *40*, 1690−1697.
(33) Bialkowski, K.; Kasprzak, K. S. *Nucleic Acids Res.* **1998**, *26*, 3194−3201.
(34) Perrin, D. D.; Dempsey, B. *Buffers for pH and Metal Ion Control*; Chapman and Hall: New York, 1974.
(35) Hunziker, M.; Ludi, A. *J. Am. Chem. Soc.* **1977**, *99*, 7370−7371.
(36) Mabrouk, P. A.; Wrighton, M. S. *Inorg. Chem.* **1986**, *25*, 526−531.
(37) DeSimone, R. E.; Drago, R. S. *J. Am. Chem. Soc.* **1970**, *92*, 2343−2352.
(38) Maniatis, T.; Fritsch, E. F.; Sambrook, J. *Molecular Cloning: A Laboratory Manual*, 2nd ed.; Cold Spring Harbor Press: Plainview, NY, 1989.
(39) Maeder, M.; Zuberbühler, A. D. *Anal. Chem.* **1990**, *62*, 2220.
(40) Yang, I. V.; Thorp, H. H. *Inorg. Chem.* **2000**, *39*, 4969−4976.
(41) Willit, J. L.; Bowden, E. F. *J. Phys. Chem.* **1990**, *94*, 8241−8246.
(42) Rudolph, M.; Reddy, D. P.; Feldberg, S. W. *Anal. Chem.* **1994**, *66*, 589a.
(43) Welch, T. W.; Corbett, A. H.; Thorp, H. H. *J. Phys. Chem.* **1995**, *99*, 11757−11763.
(44) Armistead, P. M.; Thorp, H. H. *Anal. Chem.* **2000**, *72*, 3764−3770.
(45) Bock, C. R.; Connor, J. A.; Gutierrez, A. R.; Meyer, T. J.; Whitten, D. G.; Sullivan, B. P.; Nagle, J. K. *J. Am. Chem. Soc.* **1979**, *101*, 4815.
(46) Armistead, P. M.; Thorp, H. H. *Anal. Chem.* **2001**, *73*, 558−564.
(47) Binstead, R. A.; Meyer, T. J. *J. Am. Chem. Soc.* **1987**, *109*, 3287−3297.